Appl. Phys. B 80, 449–457 (2005)
DOI: 10.1007/s00340-005-1743-3

Applied Physics B
Lasers and Optics

A. ESCUER
S. JARABO✉
J.M. ÁLVAREZ

Experimental characterisation, optimisation and design of erbium-doped silica fibre lasers

Departamento de Física Aplicada—Facultad de Ciencias, Universidad de Zaragoza, Pedro Cerbuna 12, 50.009 Zaragoza, Spain

Received: 23 September 2004 /
Published online: 16 February 2005 •
© Springer-Verlag 2005

ABSTRACT A new characterisation method is described using the new theoretical model for erbium-doped silica fibre lasers (EDSFLs) based on the energy conservation principle. Using this method, we obtained absorption and emission coefficients for the lasing wavelength at lasing operating conditions. After that, an experimental procedure to deduce the spectral profiles of the absorption and emission coefficients is also presented. This procedure allows us to obtain the values of these parameters for the whole fluorescence spectrum through measurements of gain profiles under the lasing operation. Once the absorption and emission coefficients are known, the new model can be applied and a comparison with experimental results for two different laser configurations is shown. The theoretical model is proved to be accurate and in addition some equations are developed to allow the design and optimisation of EDSFLs.

PACS 42.55.Wd; 42.81.Cn

1 Introduction

Erbium-doped silica fibre amplifiers (EDSFAs) and lasers have been of great interest for applications in optical fibre communication systems. The importance of EDSFLs in these systems is based on their possible application as multiwavelength sources in wavelength division multiplexed systems for the third window [1]. In order to optimise the behaviour of these devices it is essential to dispose of accurate theoretical models, which must provide suitable values for the main features of EDSFLs. Thus, in order to validate a theoretical model, it is necessary to check its predictions with experimental features of a high number of EDSFLs. This number of experimental set-ups developed can be reduced considering lineal cavities better than ring cavities since the laser has both forward and backward amplified spontaneous emission (ASE) powers, which makes the comparison more general. The comparison is even more useful when pumping at 1480 nm instead of 980 nm because the behaviour of the erbium-doped fibre (EDF) is more valuable since the erbium laser transition is directly pumped, and then pump stimulated emission must be considered. Following this reasoning, the kind of laser cavity and the pump wavelength would be fixed and the number of different experimental configurations reduced; however, it is still possible to build many set-ups just changing the kind of mirrors, their reflectivities or the length of EDF, as we will see later. Despite these reasons, the analysis and experimental comparison of theoretical models is rarely found in the literature. Moreover, when experimental results are compared [2–7], the comparison is not general, and papers dedicated to this subject usually lock the emission wavelength a priori (by means of optical filters, fibre Bragg gratings, etc) [5–7].

Recently, we have proposed a theoretical model based on energy conservation principle [8], which can provide a good description of the laser behaviour and can predict correctly the oscillation wavelength (with or without wavelength selector). Furthermore, it could be employed to determine beforehand the fibre and cavity parameters that optimise the laser performance, but first, this model must be checked comparing its results with experimental efficiencies, threshold pump powers and oscillation wavelengths of some laser configurations.

In this paper we will carry out this comparison, showing a good agreement between theoretical and experimental values. However, before doing this comparison, the EDF employed must be experimentally characterised to determine its absorption and emission coefficients, which constitute indispensable parameters to apply our model. To do that, we develop a characterisation method based on our theoretical model that provides the absorption and emission coefficients when lasing operation is considered. That is to say, we obtain coefficients more suitable in order to model a laser device, while other characterisation methods could provide coefficients more suitable to explain the behaviour of amplifiers [9–11]. After that, we will compare experimental and theoretical values of efficiencies and threshold pump powers for several fibre lengths using two kinds of linear cavities: one with its oscillation wavelength locked by means of a fibre Bragg grating, and another cavity allowing free oscillation wavelength. Thus, with the second cavity, we will compare values of oscillation wavelengths too. Finally, it will be shown how laser cavities can be designed and optimised employing our model.

✉ Fax: +34-976-761233, E-mail: sjarabo@unizar.es

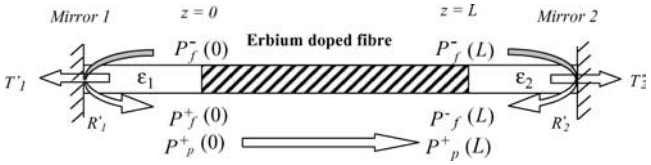

FIGURE 1 Scheme employed to develop the theoretical description of the laser

2 Experimental characterisation of EDSFLs at the oscillation wavelength

Several methods to obtain the erbium cross-sections in a silica matrix have been published [9–11]. As a result, we have several similar spectral profiles, but with high quantitative differences. Moreover, none of these methods give the cross-sections in lasing conditions. This situation led us to think of a method that provides these data at our own working conditions.

To explain the method of experimental characterisation of EDSFLs at the oscillation wavelength, we will follow the laser scheme shown in Fig. 1. This scheme is the same employed by the authors to develop the theoretical model for EDSFLs reported in Ref. [8]. As in this reference, we consider effective transmission and reflection factors, which include the transmission losses of the intracavity devices, namely $\varepsilon_1(\nu)$ and $\varepsilon_2(\nu)$. Thus, the effective reflection factors are $R_1(\lambda) = R'_1(\lambda)\varepsilon_1^2(\lambda)$ and $R_2(\lambda) = R'_2(\lambda)\varepsilon_2^2(\lambda)$, and the effective transmission factors are $T_1(\lambda) = T'_1(\lambda)\varepsilon_1(\lambda)$ and $T_2(\lambda) = T'_2(\lambda)\varepsilon_2(\lambda)$, where $R'_1(\lambda)$, $R'_2(\lambda)$, $T'_1(\lambda)$ and $T'_2(\lambda)$ are the reflection and transmission factors of mirrors 1 and 2, respectively. Moreover, it is necessary to introduce the following EDF parameters [12]

$$\gamma_\delta(\lambda) = \eta_0(\lambda)\sigma_\delta(\lambda)\bar{N}_T(\delta = a, e), \tag{1}$$

$$\beta(\lambda) = \frac{\gamma_a(\lambda) + \gamma_e(\lambda)}{\gamma_a(\lambda_p) + \gamma_e(\lambda_p)}, \tag{2}$$

$$\gamma(\lambda) = \gamma_a(\lambda_p)\beta(\lambda) - \gamma_a(\lambda), \tag{3}$$

where $\sigma_a(\lambda)$ and $\sigma_e(\lambda)$ are respectively the absorption and emission cross-sections at λ; λ_p is the pump wavelength; $\bar{N}_T$ is the mean concentration of erbium ions and $\eta_0(\lambda)$ is an overlapping factor [12].

Following this notation and taking into account that the behaviour of the erbium ion is reasonably well described considering homogeneous broadening mechanisms, it can be considered that an EDSFL oscillates at the wavelength λ_l for which the gain compensates the cavity losses. Thus, neglecting the influence of ASE power, the gain at the oscillation wavelength λ_l can be expressed by

$$G^2(L, \lambda_l)R_1(\lambda_l)R_2(\lambda_l) = 1, \tag{4}$$

where L is the EDF length. Moreover, the gain $G(z, \lambda)$ is related to the pump power $P_p^+(z, \lambda_p)$ by the expression [12]:

$$G(z, \lambda) = \exp\left[\gamma(\lambda)z\right]\left[\frac{P_p^+(z, \lambda_p)}{P_p^+(0, \lambda_p)}\right]^{\beta(\lambda)}. \tag{5}$$

So, using Eqs. 4 and 5 at $z = L$, the non-absorbed pump power (pump power at $z = L$) can be written as a function of cavity and EDF parameters as follows:

$$\beta(\lambda_l)\ln\left[\frac{P_p^+(L, \lambda_p)}{P_p^+(0, \lambda_p)}\right] + \gamma(\lambda_l)L + \frac{1}{2}\ln\left[R_1(\lambda_l)R_2(\lambda_l)\right] = 0. \tag{6}$$

As it will be seen later, parameters $\beta(\lambda)$ and $\gamma(\lambda)$ can be easily obtained for the whole spectra once they have been firstly determined for a specific wavelength. Therefore, this equation is the key of our characterisation method since it allows the experimental determination of $\beta(\lambda)$ and $\gamma(\lambda)$ at $\lambda = \lambda_l$. The procedure to obtain $\beta(\lambda_l)$ and $\gamma(\lambda_l)$ from expression (6) is simple, and it consists of measuring coupled as well as non-absorbed pump power for several EDF lengths. Then, the coefficients

$$A = -\frac{\gamma(\lambda_l)}{\beta(\lambda_l)} \quad \text{and} \quad B = -\frac{\ln[R_1(\lambda_l)R_2(\lambda_l)]}{2\beta(\lambda_l)} \tag{7}$$

can be easily determined by linear fitting to the Eq. 6. Note that this procedure can be erroneously applied if the oscillation wavelength λ_l changes. In fact, as the wavelength oscillation of an EDSFL depends on the EDF length, it is always necessary to include spectral filters (such as Bragg gratings) inside the laser cavity in order to lock the wavelength oscillation.

It is necessary to point out that the EDF can be fully characterised by $\beta(\lambda)$ and $\gamma(\lambda)$ as well as by its absorption and emission cross-sections, $\sigma_a(\lambda)$ and $\sigma_e(\lambda)$. In fact, in agreement with Eqs. 1–3, both pairs of parameters are practically equivalent in order to characterise the fibre. Nevertheless, $\beta(\lambda)$ and $\gamma(\lambda)$ are preferable because they can be experimentally obtained and because they are handier than $\sigma_a(\lambda)$ and $\sigma_e(\lambda)$ when theoretical models based on overlapping factors are employed. So, we can conclude that the EDSFL is characterised when parameters $\beta(\lambda)$ and $\gamma(\lambda)$ are determined.

To apply this characterisation method, the experimental set-up shown in Fig. 2 was developed. The laser is pumped

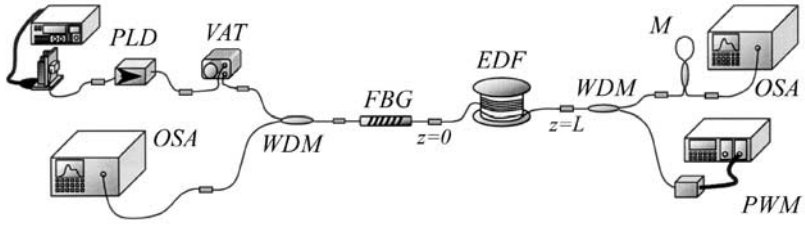

FIGURE 2 Experimental set-up used to characterise erbium-doped fibre lasers at oscillation wavelength. *PLD*: pump laser diode (1480 nm); *VAT*: variable attenuator; *WDM*: wavelength division multiplexer coupler; *FBG*: fibre Bragg grating; *M*: all-fibre mirror; *EDF*: erbium-doped fibre; *PWM*: power meter; *OSA*: optical spectrum analyser

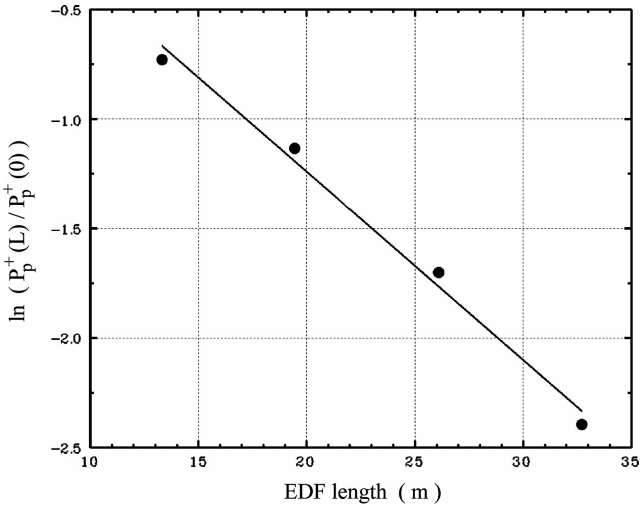

FIGURE 3 Experimental measurements fitted with Eq. 7. The experimental set-up is shown in Fig. 2

by a laser diode (Anritsu Corp., SD3F411P model) emitting around 1480 nm with the amount of pump power being regulated using a variable attenuator. The laser cavity is formed by an all-fibre mirror (50/50 coupler), a fibre Bragg grating, an EDF sample and a wavelength division multiplexer (WDM) coupler (1480/1550 nm), which is used to extract the non-absorbed pump power. The fibre Bragg grating is centred at 1556.75 nm with a full width at half-maximum around 0.3 nm and its maximum reflection factor is 0.18. The EDF is co-doped with Al, Ge and P and has an erbium concentration of 170 ppm. The core diameter is 3.8 μm, the numerical aperture is 0.17 and the lifetime of the laser level is 10.5 ms. Finally, the measurement devices employed in this set-up are a power meter (Advantest, Q82226 model) and an optical spectrum analyser (OSA, Hewlett-Packard, 70950A model).

Experimental results obtained with this set-up are shown in Fig. 3. The oscillation wavelength was $\lambda_l = 1556.68$ nm. At this wavelength, measured effective reflection factors were $R_1(\lambda_l) = 0.165$ and $R_2(\lambda_l) = 0.400$, and fitting coefficients were $A = -0.0859\ \mathrm{m}^{-1}$ and $B = 0.535$. Therefore, with the Eq. 7 we get:

$$\beta(\lambda_l) = 2.54 \quad \text{and} \quad \gamma(\lambda_l) = 0.218 m^{-1} \tag{8}$$

Once $\beta(\lambda)$ and $\gamma(\lambda)$ have been obtained for a specific wavelength, we could apply this characterisation method for every wavelength along the gain spectrum of the erbium ion to determine the spectral profiles of the parameters $\beta(\lambda)$ and $\gamma(\lambda)$. However, in order to do that, it would be necessary to place very stable tuneable filters with a wide spectral range. Moreover, applying this method to every wavelength of the erbium spectrum would be excessively tedious. To avoid this procedure and taking into account that $\beta(\lambda)$ and $\gamma(\lambda)$ only depend on EDF features, we will develop in the next section a simpler experimental procedure to obtain these parameters based on spectral gain measurements. With these measurements, spectral profiles of $\beta(\lambda)$ and $\gamma(\lambda)$ will be determined. Finally, as a correction, we will impose over them the values obtained previously at the oscillation wavelength λ_l to obtain the definitive spectral values of $\beta(\lambda)$ and $\gamma(\lambda)$.

3 Spectral characterisation of EDSFLs

To measure the spectral profiles of $\beta(\lambda)$ and $\gamma(\lambda)$, the experimental set-up shown in Fig. 4 has been used, where in contrast to Fig. 2, the all-fibre mirror has been substituted by a fibre Bragg grating. This second fibre Bragg grating works centred at 1556.60 nm with a full width at half-maximum around 0.2 nm and maximum reflection factor of 0.86. Since in this configuration both cavity mirrors are fibre Bragg gratings and their reflection profiles overlap, the EDSFL will oscillate at some intermediate wavelength; concretely, at 1556.68 nm. Finally, a WDM coupler is introduced inside the laser cavity to avoid the influence of the non-absorbed pump power on the measurements made by the OSA.

The experimental procedure is based on the spectral gain measurement of the EDSFL, employing a light emitting diode (LED) as the signal power source and measuring the amplified signal power with an OSA. The power emitted by the LED is low enough to consider populations of the erbium energy levels unmodified, but high enough to allow accurate measurements as it was checked by means of synchronous detection based on the use of a lock-in amplifier. Note that this method can not provide correct measurements at oscillation wavelength since signal power overlaps laser power. Thus, it is possible to have the whole gain profile measured, except around the oscillation wavelength. In fact, the value of $G(L, \lambda)$, that is to say, the gain of an EDF sample with length L for every wavelength $\lambda \neq \lambda_l$, can be easily obtained. For this purpose, two measurements with a sample of EDF of length L will be made: the power when the LED is on, $P_{\mathrm{on}}(L, \lambda)$ and the power when the LED is off, $P_{\mathrm{off}}(L, \lambda)$. Later two similar measurements but introducing an EDF sample of very short length will be made: the power when the LED is on, $P_{\mathrm{on}}(0, \lambda)$ and the power when the LED is off, $P_{\mathrm{off}}(0, \lambda)$. Note that these two measurements are necessary to measure the power emitted by the LED taking into account insertion losses of fibre splices. Thus, we have:

$$G(L, \lambda) = \frac{P_{\mathrm{on}}(L, \lambda) - P_{\mathrm{off}}(L, \lambda)}{P_{\mathrm{on}}(0, \lambda) - P_{\mathrm{off}}(0, \lambda)}, \quad \forall \lambda \neq \lambda_l. \tag{9}$$

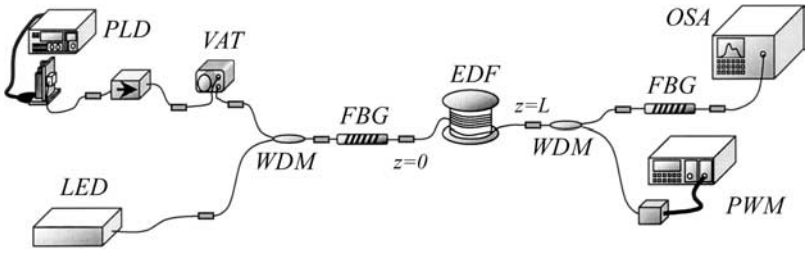

FIGURE 4 Experimental set-up used to carry out the spectral characterisation of erbium-doped fibre lasers by mean of gain measurements. *PLD*: pump laser diode (1480 nm); *LED*: light emission diode (signal); *VAT*: variable attenuator; *WDM*: wavelength division multiplexer coupler; *FBG*: fibre Bragg grating; *EDF*: erbium-doped fibre; *PWM*: power meter; *OSA*: optical spectrum analyser

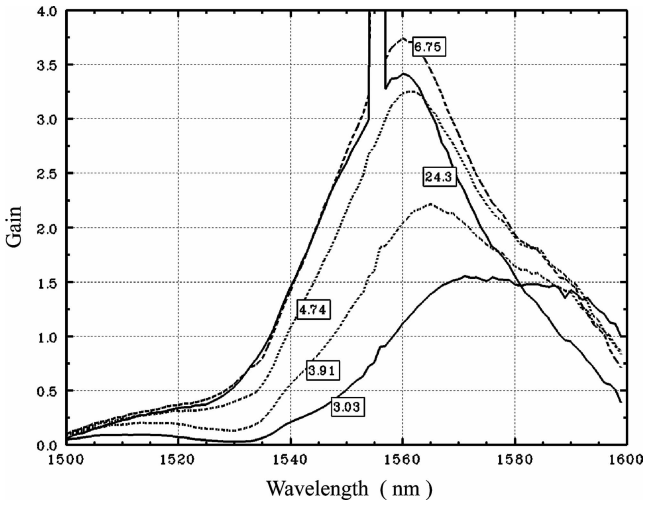

FIGURE 5 Gain spectra profiles measured with the experimental set-up shown in Fig. 4 employing several pump powers. Each spectrum profile is labelled with its pump power value in milliwatts

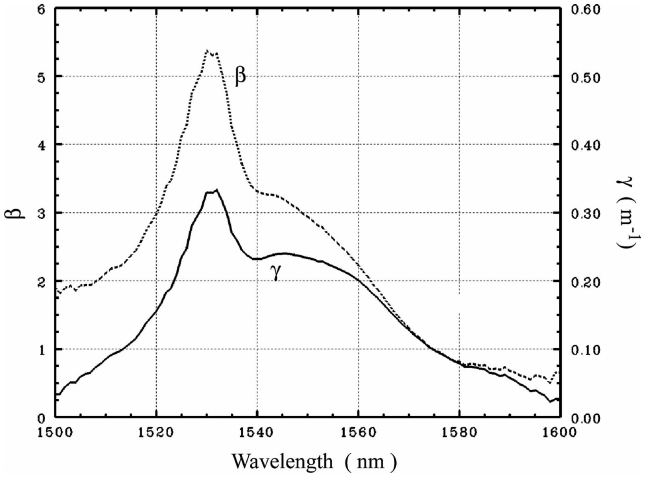

FIGURE 6 Spectra profiles of parameters β and γ obtained with pump power at 1480 nm. These profiles were obtained after interpolating at the oscillation wavelength and after recalculating each spectrum to make values at oscillation wavelength coincide with those shown in Eq. 8

Once we have an expression for the gain, we can use Eq. 5, which can be rewritten as follows:

$$\ln\left[G(L,\lambda)\right] = \beta(\lambda)\ln\left[\frac{P_{\mathrm{p}}^{+}(L,\lambda_{\mathrm{p}})}{P_{\mathrm{p}}^{+}(0,\lambda_{\mathrm{p}})}\right] + \gamma(\lambda)L. \tag{10}$$

With this equation, parameters $\beta(\lambda)$ and $\gamma(\lambda)$ can be easily determined by linear fitting when gain and ratio between coupled and non-absorbed pump power are measured for several EDF lengths or for several input pump powers. To simplify the experimental procedure, it is more interesting to work varying the input pump powers instead of the EDF length since in that case laser cavity must not be modified. Thus, choosing a resolution of 1 nm, several spectral gain measurements for several input pump powers and an EDF length of 19.5 m are shown in Fig. 5. Fitting these measurements to Eq. 10 for every wavelength, the spectral shape of the parameters $\beta(\lambda)$ and $\gamma(\lambda)$ is determined. Finally, imposing to these profiles the values at the oscillation wavelength shown in Eq. 8, which were obtained through measurements in laser regime conditions, the $\beta(\lambda)$ and $\gamma(\lambda)$ spectra are obtained. These spectra are gathered in Fig. 6.

Note that although the experimental procedure exposed is simple and, as it will be seen later, provides correct values of the parameters $\beta(\lambda)$ and $\gamma(\lambda)$, it does not work well for wavelengths near the oscillation wavelength, where laser power overlaps LED power. However, this problem affects only a very narrow wavelength range and on the other hand values of $\beta(\lambda)$ and $\gamma(\lambda)$ at oscillation wavelength are well determined. Therefore, we can conclude that the definitive profiles of $\beta(\lambda)$ and $\gamma(\lambda)$ can be corrected by interpolation, leading to a good characterisation of the EDF.

4 Comparison with experimental results

To check the validity of the obtained profiles as well as our model's good operation, a comparison between theoretical and experimental results will be made. For this purpose, we will begin by applying the approach of negligible spontaneous emission to the expressions of the efficiency and threshold power developed in Ref. [8]. Then, we will apply the expressions (4) and (6) to obtain simpler analytic equations of the most important laser features:

$$\eta^{+}(L,\lambda) = \frac{\lambda_{\mathrm{p}}}{\lambda_{\mathrm{l}}}\frac{1-\frac{P_{\mathrm{p}}^{+}(L)}{P_{\mathrm{p}}^{+}(0)}}{\left[1+\sqrt{\frac{R_2(\lambda)}{R_1(\lambda)}}\right]}, \tag{11}$$

$$\eta^{-}(L,\lambda) = \frac{\lambda_{\mathrm{p}}}{\lambda_{\mathrm{l}}}\frac{1-\frac{P_{\mathrm{p}}^{+}(L)}{P_{\mathrm{p}}^{+}(0)}}{\left[1+\sqrt{\frac{R_1(\lambda)}{R_2(\lambda)}}\right]}, \tag{12}$$

$$P_{\mathrm{th}}(L,\lambda) = \frac{P_{\mathrm{p}}^{\mathrm{th}}\frac{\gamma_{\mathrm{p}}}{\gamma_{\mathrm{a}}(\lambda)+\gamma_{\mathrm{e}}(\lambda)}\left\{\gamma_{\mathrm{a}}(\lambda)L-\frac{1}{2}\ln\left(R_1(\lambda)R_2(\lambda)\right)\right\}}{1-\frac{P_{\mathrm{p}}^{+}(L)}{P_{\mathrm{p}}^{+}(0)}}, \tag{13}$$

where λ_{p} is the pumping wavelength, $P_{\mathrm{p}}^{\mathrm{th}}$ is the parameter defined in Refs. [8] and [12] and $\gamma_{\mathrm{p}} \equiv \gamma_{\mathrm{a}}(\lambda_{\mathrm{p}})$.

Note that to apply any of the expressions (11)–(13), it is necessary to know, besides the profiles of $\beta(\lambda)$ and $\gamma(\lambda)$, the oscillation wavelength. It is important to keep in mind that the oscillation wavelength cannot be determined in the approach of negligible ASE, since the spectral shape of the ASE within the doped fibre is not considered versus the power values at the oscillation wavelength. For this reason, when other authors want to verify a theoretical model which uses this approach, spectral filters or Bragg gratings are introduced inside the cavity to force the system to oscillate at a previously determined wavelength. In our case, to solve this aspect, we will take advantage of the fact that our original model actually preserves the spectral information, and we will use the relationship between the spectral profiles of γ and β and the cavity parameters given by (6).

Since an homogeneous medium is considered, gain can only achieve losses for $\lambda = \lambda_{\mathrm{l}}$, and therefore Eq. 4 takes values under unity for any other wavelength of the spectrum. Following the same reasoning, function $G^2(L,\lambda)R_1(\lambda)R_2(\lambda)$

takes negative values for any wavelength except for the oscillation wavelength, for which it becomes null. So, this function reaches its maximum at $\lambda = \lambda_l$, and therefore:

$$2L\frac{\mathrm{d}\gamma(\lambda)}{\mathrm{d}\lambda} + 2\ln\frac{P_p(L,\lambda_p)}{P_p(0,\lambda_p)}\frac{\mathrm{d}\beta(\lambda)}{\mathrm{d}\lambda} + \frac{\mathrm{d}}{\mathrm{d}\lambda}\{\ln[R_1(\lambda)R_2(\lambda)]\}\Big|_{\lambda=\lambda_l} = 0. \quad (14)$$

Although it seems that Eq. 6 as well as Eq. 14 could be used to calculate λ_l, note that the pump power at the end of the doped fibre is not known. Thus, using both expressions we get finally the following expression:

$$\frac{\mathrm{d}}{\mathrm{d}\lambda}\left\{\frac{2\gamma(\lambda)L + \ln[R_1(\lambda)R_2(\lambda)]}{\beta(\lambda)}\right\}\Big|_{\lambda=\lambda_l} = 0, \quad (15)$$

which gives the oscillation wavelength of a laser configuration starting from the cavity characteristics (L, R_1 andR_2) and the doped fibre parameters (γ and β). Once the lasing wavelength and the spectral profiles of β and γ have been obtained, analytical Eqs. 11–13 can be applied and compared with experimental results. First, they will be applied to the experimental laser configuration of Fig. 2, which was the one used earlier to obtain the values of β and γ at the oscillation wavelength. The parameter values of the EDF chosen for experimental configurations from here on, are: $\gamma_p = 0.23\ \mathrm{m}^{-1}$, $\gamma_e(\nu_p) = 0.11\ \mathrm{m}^{-1}$, $\tau = 10.5$ ms, $\bar{N}_T = 2.4 \times 10^{24}\ \mathrm{m}^{-3}$ and $\rho = 1.9\ \mu$m. In Figs. 7–9 it can be seen how the theoretical model deduced in Ref. [8], describes correctly the experimental behaviour of the laser even after neglecting the ASE.

Although the values of $\beta(\lambda)$ and $\gamma(\lambda)$ obviously have an influence on all the laser features, the best way to prove the good operation of these profiles is to predict with them the lasing wavelength in a free oscillation configuration (without spectral filters). In order to do that, the full model described in Ref. [8] as well as Eq. 15 can be used. This reasoning comes from the fact that the spectral resolution considered in the calculus of the profiles is just 1 nm. Then, a little variation in the calculus of the oscillation wavelength makes the prediction

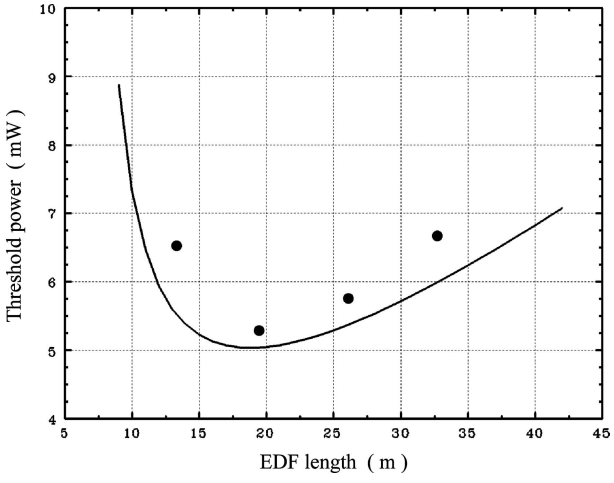

FIGURE 7 Comparison between the threshold pump power given by Eq. 13 and the experimental values (*circle dots*) obtained with the set-up shown in Fig. 2

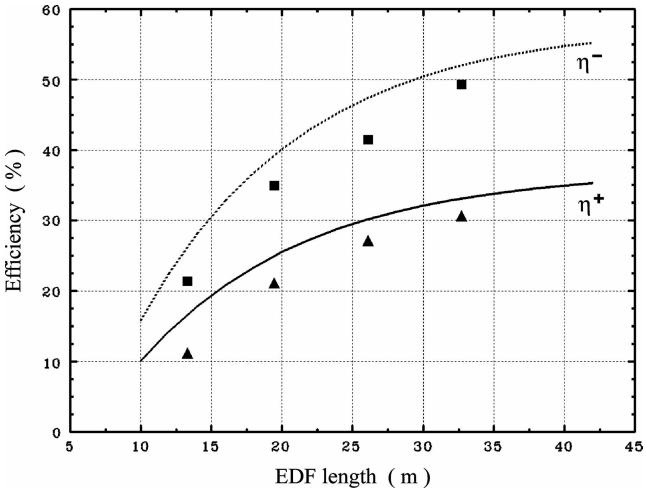

FIGURE 8 Theoretical values of forward (η^+, Eq. 11, *triangle dots*) and backward propagating efficiency (η^-, Eq. 12, *square dots*) compared with experimental measurements carry out with the set-up of Fig. 2

jump to the next or to the previous nanometer, which results more remarkable than for instance a slight increase in the value of the efficiency.

Furthermore, it seems reasonable that the developed equations give an accurate description for the laser configuration of Fig. 2, since this is the one used to deduce the values of β and γ for the oscillation wavelength. Note that this situation would only indicate that an auto-consistent theoretical model has been developed, which actually is not the purpose. To prove that this is not the case, we will apply now our model (together with the spectral profiles of $\beta(\lambda)$ and $\gamma(\lambda)$ obtained with the new method developed in this paper), to another experimental configuration with free oscillation. This experimental configuration was already described in detail in Ref. [13] and it is the one shown in Fig. 10. Here we will only remember as its main characteristics that the effective reflectivities at

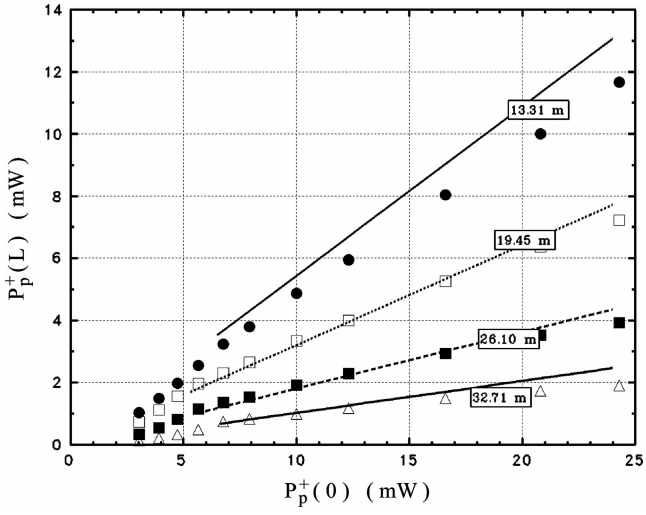

FIGURE 9 Theoretical (*lines*) and experimental (*dots*) values of the pump power at $z = L$ versus the pump power coupled into the fibre. Theoretical values were computed by means of Eq. 6 and experimental values were measured in the set-up of Fig. 2. Each line is labelled with the erbium-doped fibre length used in the comparison

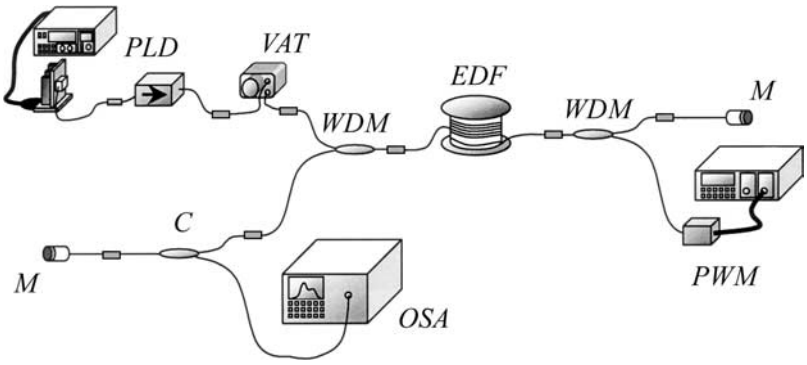

FIGURE 10 Experimental set-up employed to check our model in erbium-doped fibre lasers with free oscillation. Each mirror (labelled as *M*) is made with a fibre connector coated with aluminium (thickness of 100 nm) and the coupler 95/5 (labelled as *C*) is necessary to extract the laser emission power out of the cavity. *PLD*: pump laser diode (1480 nm); *VAT*: variable attenuator; *WDM*: wavelength division multiplexer coupler; *EDF*: erbium-doped fibre; *PWM*: power meter; *OSA*: optical spectrum analyser

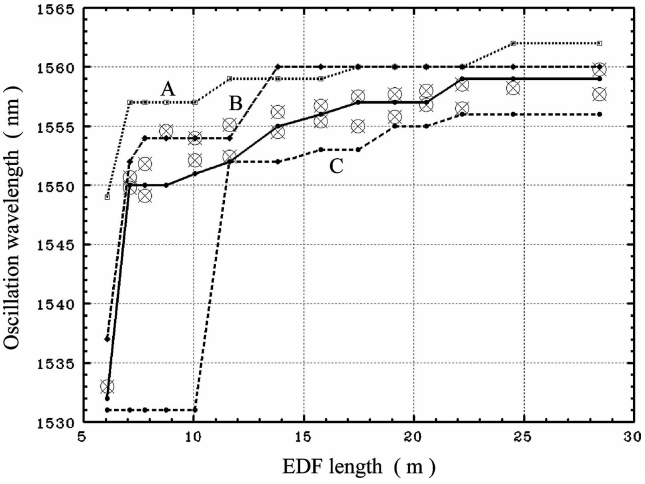

FIGURE 11 Comparison between experimental (*crossed circles*) and theoretical (*lines*) oscillation wavelengths obtained for the set-up shown in Fig. 10. Theoretical values were deduced using the profiles of parameters β and γ shown in Fig. 6 (*solid line*) and also values of parameters β and γ published by other authors: *A* Ref. [9]; *B* Ref. [10]; *C* Ref. [11]

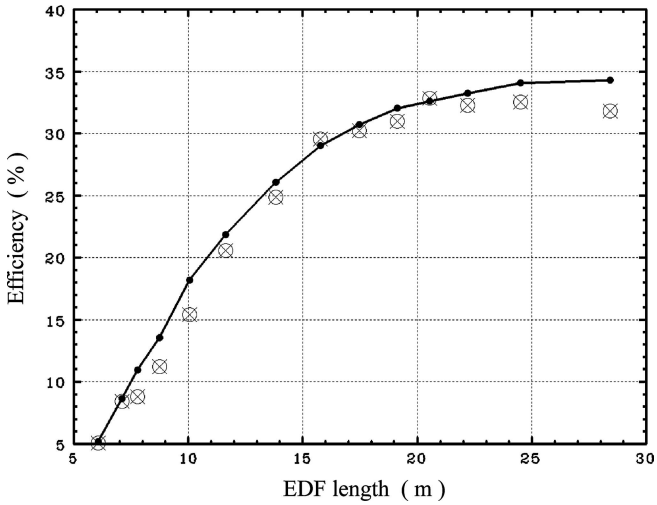

FIGURE 12 Comparison between experimental (*crossed circles*) and theoretical (*solid line*) backward propagating efficiency obtained for the set-up shown in Fig. 10. Theoretical values were obtained employing the spectral profiles of parameters β and γ shown in Fig. 6

1556 nm are $R_1 = 23.7\%$ and $R_2 = 42.0\%$ and also that the mirrors used are aluminium-coated fibre connectors with a layer of 100 nm. These mirrors have no dependence on wavelength but as a consequence of their thickness, they do not let pass the laser power outside the cavity (because it is absorbed), and therefore a 95/5 coupler had to be introduced to extract it.

Since no spectral filters are introduced in the cavity, every time the doped fibre length is changed, so does the lasing wavelength by virtue of (6). In Fig. 11 a comparison between experimental and theoretical results for the oscillation wavelength versus EDF length is shown. In this figure we can see four curves, which correspond to the calculus made with our model but introducing four different spectral profiles of $\beta(\lambda)$ and $\gamma(\lambda)$: firstly the ones deduced in this paper and shown in Fig. 6, and then another three published by other authors [9–11]. It can be noticed in Fig. 11, that the curve that better adjusts to the experimental results is the one obtained using the $\beta(\lambda)$ and $\gamma(\lambda)$ profiles deduced in this paper. Using again these profiles together with Eqs. 11–13, for the new experimental configuration, we obtain the results plotted in Figs. 12–14.

It is necessary to clarify that all the equations and theoretical expressions shown in this paper refer to laser emission powers and efficiencies inside the cavity, in particular, at the ends of the doped fibre. Thus if we want to know the values outside the cavity, we must multiply the results obtained inside by the effective transmission of the mirrors. However, in this paper we have proceeded inversely, and the powers

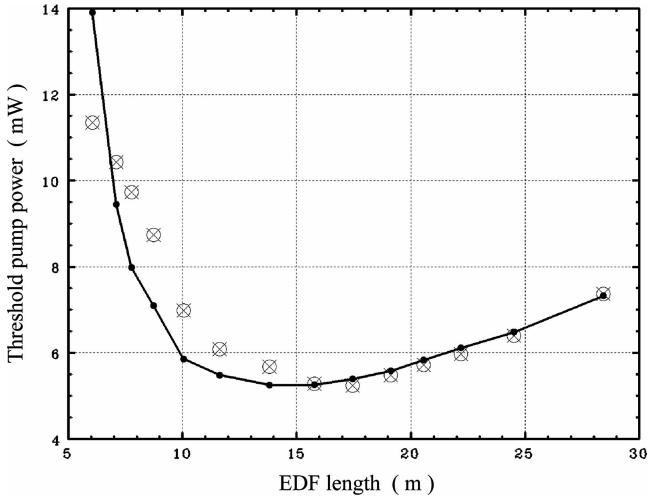

FIGURE 13 Comparison between experimental (*crossed circles*) and theoretical (*solid line*) threshold pump power obtained for the set-up shown in Fig. 10. Theoretical values were obtained employing the spectral profiles of parameters β and γ shown in Fig. 6

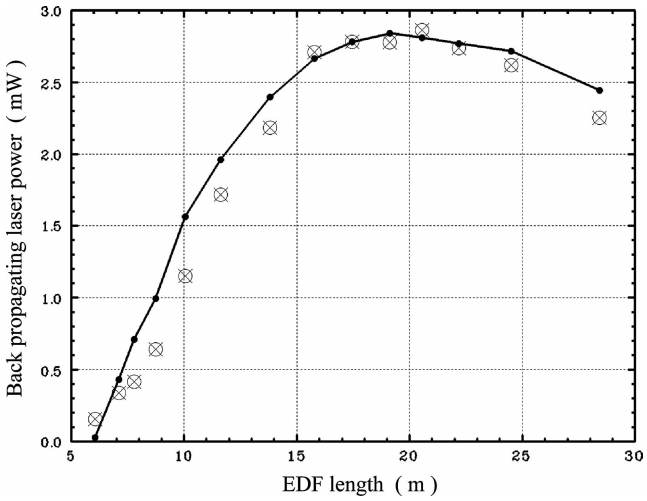

FIGURE 14 Comparison between experimental (*crossed circles*) and theoretical (*solid line*) back propagating laser power obtained for the set-up shown in Fig. 10. Theoretical values were obtained employing the spectral profiles of parameters β and γ shown in Fig. 6

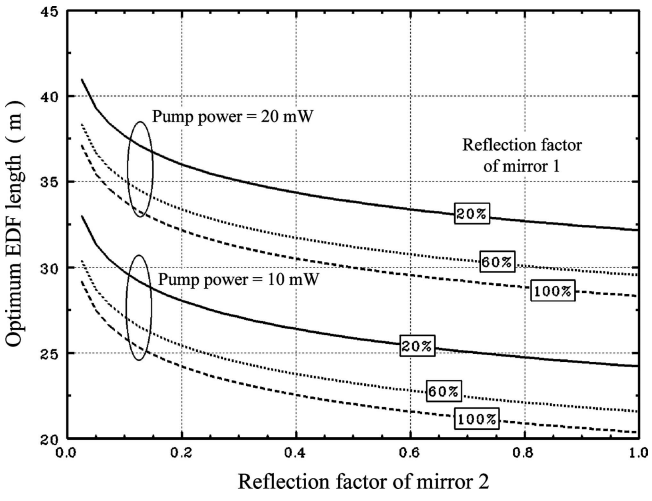

FIGURE 16 Optimum EDF length that maximises laser emission power plotted as a function of the reflection factor of mirror (*2*). Several reflection factors of mirror (*1*)and pump powers have been considered

measured outside the cavity have been divided by the effective transmissions for each laser configuration in order to compare between theory and experience. Concretely, in the case of the experimental points obtained for the laser configuration of Fig. 10, it has been also kept in mind the influence of the internal fibre splices, due to the fact that the EDF was formed by several samples. Since they are internal losses, the transmission losses produced by this splices were not included in the effective transmissions or reflections of the mirrors, and that is the reason why some differences between the experimental points showed here and the ones reported in Ref. [13] exist.

5 Design and optimisation of laser configurations

Once proved that the new model developed in Ref. [8] follows satisfactorily the experimental behaviour, we can go beyond and try to deduce equations and parameters useful to design and optimise laser configurations. The idea consists of knowing a priori as many data as possible of a laser configuration, and then starting from there, to optimise this information to build a laser with the wanted characteristics.

Thus, we would begin by defining the threshold doped fibre length. This parameter is defined as the doped fibre length below which, whatever the introduced pump power is, laser oscillation never occurs. The way to obtain an expression for the threshold length is just to equal to zero the denominator of the expression of the power threshold (13) and applying (6) to conclude that:

$$L_{\mathrm{th}}(\lambda_{\mathrm{l}}) = -\frac{1}{2\gamma(\lambda_{\mathrm{l}})} \ln\left(R_1(\lambda_{\mathrm{l}})R_2(\lambda_{\mathrm{l}})\right), \tag{16}$$

where the oscillation wavelength must be deduced starting from Eq. 15. In Fig. 15 some curves with the dependence of this parameter on the mirror reflections are shown.

Equation 16 can be physically reasoned too taking into account that gain grows with input pump power, and therefore maximum gain is obtained when $P_{\mathrm{p}}^{+}(0, \lambda_{\mathrm{p}}) \to \infty$. This condition is the most favourable in order to verify the oscillation condition determined by Eq. 4. Then, from Eq. 5, it is clear that $\exp[\gamma(\lambda)L]$ is the maximum gain that one sample of length L can provide. Consequently, as $\exp[\gamma(\lambda)L]$ increases with L and as it is necessary that gain reaches the value $[R_1(\lambda_{\mathrm{l}})R_2(\lambda_{\mathrm{l}})]^{-1/2}$ imposed by Eq. 4, then it is easy to see that a threshold length exists, which is expressed by Eq. 16.

With the expression of the threshold length, the most important features of the laser can be rewritten as follows:

$$G(L, \lambda) = \exp(\gamma(\lambda)L) \exp\left(-\frac{\gamma(\lambda_{\mathrm{l}})}{\beta(\lambda_{\mathrm{l}})}\beta(\lambda)(L - L_{\mathrm{th}})\right), \tag{17}$$

$$\eta^{+}(L) = \frac{\lambda_{\mathrm{p}}}{\lambda_{\mathrm{l}}} \frac{1 - \exp\left(-\frac{\gamma}{\beta}(L - L_{\mathrm{th}})\right)}{1 + R_2 \exp(\gamma L_{\mathrm{th}})}, \tag{18}$$

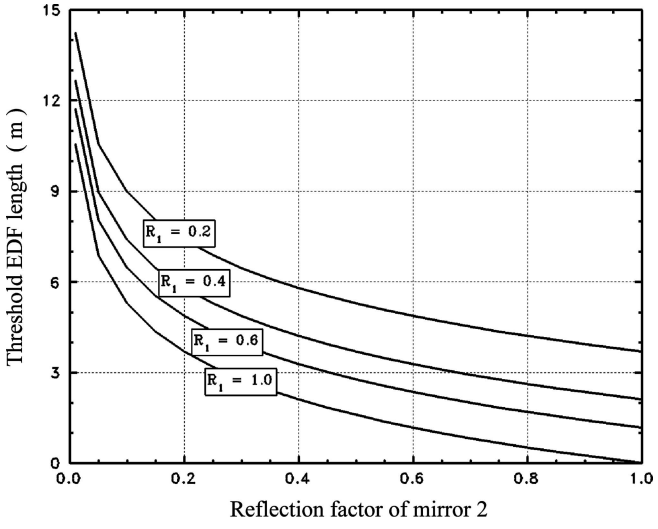

FIGURE 15 Theoretical threshold EDF length plotted as a function of the reflection factor of mirror (*2*) and computed for several reflection values of mirror (*1*)

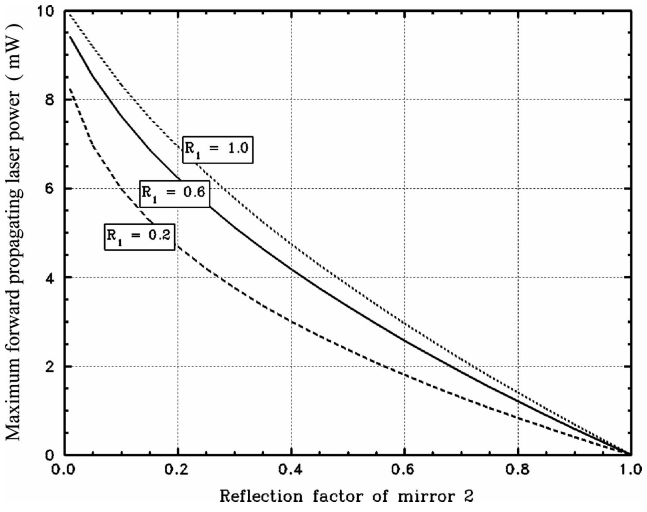

FIGURE 17 Maximum forward propagating laser power plotted as a function of the reflection factor of mirror (*2*). These values of laser power are obtained outside the cavity considering no internal losses in mirrors and once the optimum EDF length of Fig. 16 is introduced. Results for several reflection factors of mirror (*1*) and an introduced pump power of 20 mW are shown

$$\eta^{-}(L) = \frac{\lambda_p}{\lambda_l} \frac{1 - \exp\left(-\frac{\gamma}{\beta}(L - L_{th})\right)}{1 + R_1 \exp(\gamma L_{th})}, \tag{19}$$

$$P_{th}(L) = \frac{P_p^{th} \frac{\gamma_p}{\gamma_a + \gamma_e} [\gamma_a L + \gamma L_{th}]}{1 - \exp\left(-\frac{\gamma}{\beta}(L - L_{th})\right)}, \tag{20}$$

$$P^{\pm}_{laser}(L) = \eta^{\pm}(L) \cdot [P_p^{+}(0) - P_{th}(L)]. \tag{21}$$

Starting from these equations, laser configurations can be optimised, for instance, as a function of the EDF length or as a function of the reflection factors of the cavity. Logically enough, laser optimisation will only make sense when oscillation wavelength is locked. So, we are going to consider that our laser cavity has got one filter, which locks λ_l. Thus, differentiating Eqs. 18 or 19 over the doped fibre length it can be seen that both efficiencies reach their maximum when $L \to \infty$, taking then a value on the whole equivalent to the quantum efficiency. Working in a similar way but with the threshold power (20), we get an expression that, although simple, requires numerical resolution:

$$\exp\left(\frac{\gamma}{\beta}(L - L_{th})\right) - 1 = \frac{\gamma}{\beta}(L - L_{th}) + \frac{\gamma \gamma_p}{\gamma_a} L_{th}. \tag{22}$$

However, when we try to optimise the EDF length, which maximizes the laser emission power, we obtain then an analytic expression:

$$L_{opt} = L_{th} + \frac{\beta}{\gamma} \ln\left[\frac{P_p^{+}(0)}{P_p^{th}} \frac{\gamma}{\gamma_a} \frac{\alpha_p}{\gamma_p}\right], \tag{23}$$

where $\alpha_p \equiv \gamma_p + \gamma_e(\nu_p)$. This parameter determines for any laser cavity, which is the doped fibre length that makes maximum the laser emission power (as shown in Fig. 16). The value of this power in the forward case is given by:

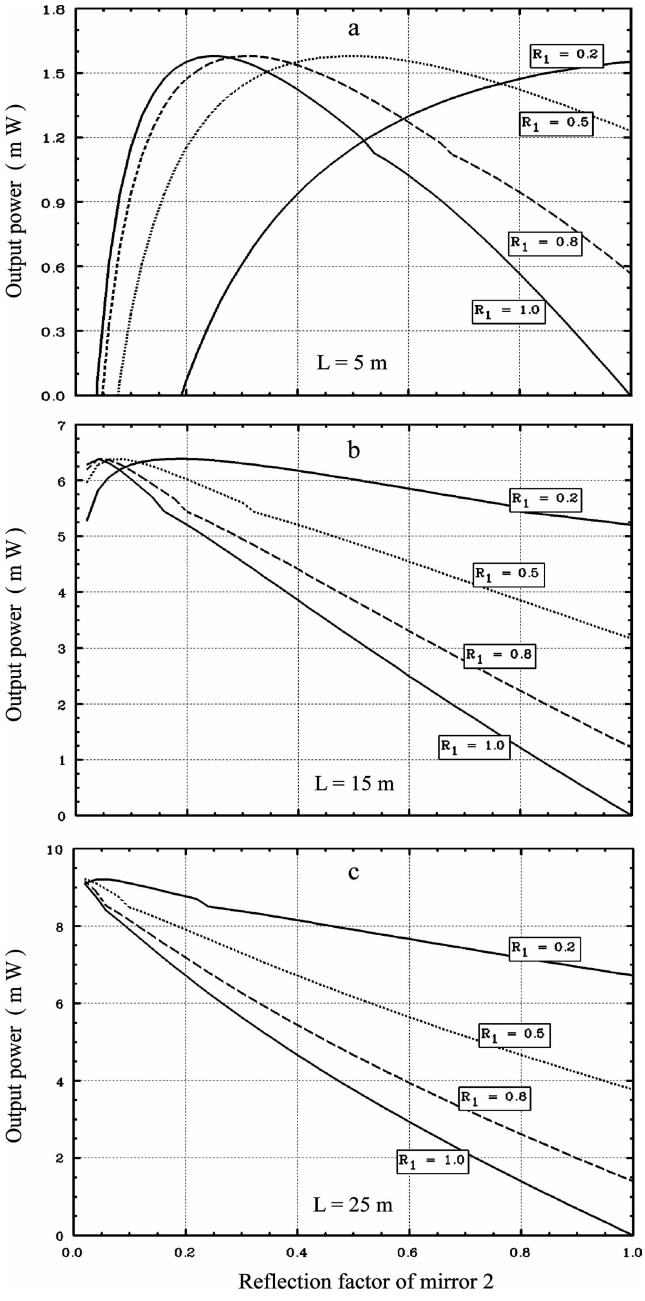

FIGURE 18 Total (back plus forward propagating) laser emission power outside the cavity plotted as a function of the reflection factor of mirror (*2*). Several reflection factors of mirror (*1*) have been considered and no internal losses in the mirrors have been introduced. The EDF length is in each case: **a** 5 m, **b** 15 m and **c** 25 m

$$P^{+}_{laser,\,máx} = \frac{\lambda_p}{\lambda_l} \frac{P_p(0) - P_p^{th} \frac{\gamma_p}{\alpha_p} \left[\gamma_p L_{th} + \gamma_a \left(\frac{1}{\gamma} + \frac{L_{opt} - L_{th}}{\beta}\right)\right]}{1 + R_2 \exp[\gamma L_{th}]}, \tag{24}$$

where the dependence on the reflection factors of the cavity is included in L_{th}. In Fig. 17 we have plotted the maximum forward propagating laser power outside the cavity in the unusual and hypothetical case that mirror 2 has no internal losses, that is, the values obtained from Eq. 24 multiplied by

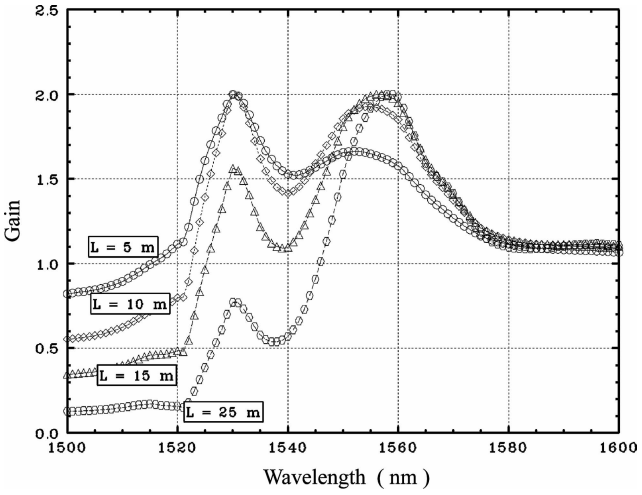

FIGURE 19 Spectral gain profiles computed by means of Eq. 17. Reflection factors of 0.5 for both mirrors and EDF lengths of 5, 10, 15 and 25 m have been considered

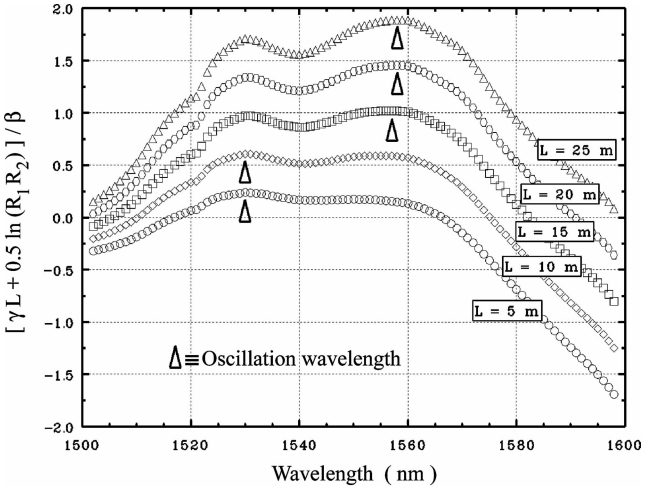

FIGURE 20 Spectral profiles of the function $[\gamma L+0.5\ \ln(R_1 R_2)]/\beta$. Reflection factors of 0.5 for both mirrors and EDF lengths of 5, 10, 15, 20 and 25 m have been considered. The laser oscillates at the wavelength that maximises this function

$(1 - R_2)$. In the case of laser configurations where forward and backward propagating powers are extracted simultaneously, it could be useful to know the total power outside the cavity obtained as a function of both reflection factors and of the doped fibre length (Fig. 18). For this purpose, Eqs. 21, 24 and another similar to 24 but obtained for backward propagating laser power have been used and no internal losses have been considered for both mirrors.

As expected, these equations help us to predict the experimental behaviours of a laser cavity before building it. However, sometimes it can also be useful to represent not measurable parameters to have a better knowledge of the internal working of our laser configuration in order to understand better the theoretical model or in order to predict future improvements. Thus, for instance, we can plot the gain spectra (Fig. 19) or the numerical function whose maximum determines the oscillation wavelength (Fig. 20).

6 Conclusions

Working with our theoretical model based on energy conservation principle, we have developed and applied a new characterisation method to obtain the absorption and emission coefficients of an erbium doped fibre (EDF), which is employed as amplifying medium of several linear cavity lasers. This method is not limited at the oscillation wavelength, and in consequence absorption and emission coefficients are determined for every wavelength of the erbium gain profile. Moreover, our characterisation method provides absorption and emission coefficients in lasing conditions, that is to say, at our own working conditions. Thus, it is proved that our method can be used to characterise EDFs better than other methods previously published.

Experimental values of efficiencies and threshold pump powers for several fibre lengths were measured using two kinds of linear cavities: one with its oscillation wavelength locked by means of a fibre Bragg grating, and another cavity allowing free oscillation wavelength. So, with the second cavity, values of oscillation wavelength versus EDF length were measured. Later, using the EDF coefficients experimentally characterised, we carried out the comparison between these experimental measurements and the theoretical results provided by our model, showing a good agreement between them and, therefore, confirming the correctness of our theoretical model based on energy conservation.

Finally, some additional equations based on our model have been developed to allow the optimisation and design of EDSFLs.

ACKNOWLEDGEMENTS The authors are grateful to A. García de Cáceres for his valuable comments. This work was supported by the national research program Programa Nacional de Tecnología de la Información y de las Comunicaciones (PRONTIC, Project. No. TIC99-0942).

REFERENCES

1 A. Bellemare, Prog. Quantum Electron. **27**, 211 (2003)
2 P. Franco, M. Midrio, A. Tozzato, M. Romagnoli, F. Fontana, J. Opt. Soc. Am. B **11**, 1090 (1994)
3 A. Cucinotta, S. Dallargine, S. Selleri, C. Zilioli, M. Zoboli, Opt. Commun. **141**, 21 (1997)
4 A. Cucinotta, S. Selleri, L. Vincetti, M. Zoboli, Opt. Commun. **156**, 264 (1998)
5 Th. Pfeiffer, H. Schmuck, H. Bülow, IEEE Photonics Technol. Lett. **4**, 847 (1992)
6 J.P. Burger, P.L. Swart, S.J. Spammer, P.V. Bulkin, Opt. Eng. **36**, 593 (1997)
7 A. Bellemare, M. Karásek, C. Riviere, F. Babin, G. He, V. Roy, G.W. Schinn, IEEE J. Sel. Top. Quantum Electron. **7**, 22 (2001)
8 A. Escuer, S. Jarabo, J.M. Álvarez, J. Mod. Opt. **52**, 655 (2005)
9 S. Jarabo, J.M. Álvarez, Appl. Opt. **37**, 2288 (1998)
10 J.C. Martín, J.M. Álvarez, M.A. Rebolledo, J. Mod. Opt. **48**, 1421 (2001)
11 E. Desurvire, J.R. Simpson, J. Lightwave Technol. **7**, 835 (1989)
12 A. Escuer, S. Jarabo, J.M. Álvarez, Opt. Commun. **187**, 107 (2001)
13 A. Escuer, S. Jarabo, J.M. Álvarez, Fiber Integr. Opt. **17**, 255 (1998)